Supporting Information

Highly Conductive and Permeable Nanocomposite Ultrafiltration Membranes Using Laser-Reduced Graphene Oxide

Anthony P. Straub[*], David S. Bergsman, Bezawit A. Getachew, Liam M. Leahy, Jatin J. Patil, Nicola Ferralis, and Jeffrey C. Grossman[*]

Department of Materials Science and Engineering, Massachusetts Institute of Technology, Cambridge, Massachusetts 02139, United States

*Corresponding authors:
Anthony P. Straub, E-mail: anthony.straub@colorado.edu, Phone: (+1) 303-735-4575
Jeffrey C. Grossman, E-mail: jcg@mit.edu, Phone: (+1) 617-324-3566

Supplementary Materials and Methods

Materials and Chemicals

Graphene oxide (GO) was purchased from Graphenea (Cambridge, MA) in a 4 g/L solution. Polyethersulfone (PES) ultrafiltration support membranes with a 0.2 µm pore size and 47 mm diameter were purchased from Sterlitech (Kent, WA). *p*-Phenylenediamine and chemically reduced GO were purchase from Sigma Aldrich.

Deposition and Laser Reduction of Graphene Oxide.

To create laser-reduced GO coatings, GO solutions of various concentrations (as indicated from the loading in the main text) were prepared by adding 4 g/L graphene oxide stock solution to 50 mL DI water. Samples were bath ultrasonicated for 10 minutes and then vacuum deposited onto the support PES membrane. After vacuum deposition, membranes were dried in air for 10 hours. Select membranes were subsequently laser irradiated using a CO_2 laser cutter system (VersaLASER, VLS 2.3, 10.6 µm, 25 W laser), using the following system parameters: speed of 50%, image density of 4, and laser power of 30%. Speed and laser power parameters were typically adjusted between sample to maintain high electrical conductivity.

Fabrication of the membrane was also carried out with *p*-phenylenediamine (PPD) additives to improve electrical conductivity. The fabrication procedure was identical to the GO vacuum filtration method described above, but 0.027 g of PPD were mixed with 50 mL DI water and the GO stock solution. The amount of PPD was optimized to prevent delamination of the GO layer and followed a similar concentration as was used in Hung et al.[1]

Materials Characterization

Scanning electron microscopy (SEM) images were obtained on a Zeiss Ultra 55 and a Hitachi Regulus 8100 SEM. X-tray photoelectron spectroscopy (XPS) scans were performed on a Thermo Scientific K-Alpha system, using Al Kα as an x-ray source. A spot size of 400 $µm^2$ was used. Regional scans were averaged over 10 repeated measurements using a 25 ms dwell time per eV step (pass energy 50 eV and a 0.1 eV step size). Raman spectroscopy was performed on a Horiba LabRAM 800 HR spectrometer using a 633 nm laser and a 400 nm hole. The laser was focused at ×100 under reflected illumination. Fourier transform infrared spectroscopy (FTIR) spectra were collected using a Thermo Fisher FTIR6700, a germanium attenuated total reflection (ATR) plate,

and a mercury-cadmium-telluride detector chilled with liquid nitrogen. Background scans were taken using the uncoated ATR plate. Spectra were averaged over 200 scans, with a step size of $4\,cm^{-1}$. Conductivity was measured using an MMR Variable Temperature Hall Measurement System. In each measurement, the voltage was optimized for maximum allowable current. $1\,cm^2$ samples were used. Permeability was measured using a home-built dead-end filtration test cell. Test membranes were epoxied to polyethylene terephthalate (PET) plastic rings (with a set inner diameter) to provide structural support before being sandwiched between an o-ring and sealing surface. Pressurized water was then forced through the membrane and collected onto a laboratory balance to measure the volumetric flow rate of water. Dye degradation studies were performed using Bio-logic SP-300 potentiostat in a three-electrode cell setup as shown in Figure S1 below. Thin strips of the GO were deposited into 50 mM NaCl solutions, so that electrolyte did not make contact with alligator clips. A platinum wire was used as the counter electrode and an Ag/AgCl electrode, purchased from Fischer Scientific (Fisherbrand accumet, glass body) was used as a voltage reference. Electrochemical impedance spectroscopy was used to measure the series resistance of the cell before running chronoamperometry (8 V applied).

Figure S1. Photo of electrochemical dye degradation setup.

Raman Spectroscopy Analysis

Raman spectroscopy is widely used to characterize graphitic materials (graphene, graphite, disordered graphite, defects in graphene and graphite, amorphous and nanostructured carbon, etc.).

Raman spectra of most carbon allotropes contain a few strong bands in the 1000-2000 cm^{-1} region and a few other weaker bonds, regardless of their structure. What allows distinction between different types of carbonaceous materials is the shape, intensity, and position of these few peaks.

To characterize complex graphitic materials (other than pure graphene and bulk graphite) using Raman spectroscopy, Ferrari *et al* introduced a phenomenological three-stage classification of disorder.[2]   The stages range from graphite to nanocrystalline graphite (stage 1), from nanocrystalline graphite to low sp^3 amorphous carbon (stage 2), and from low sp^3 amorphous carbon to high sp^3 amorphous carbon (stage 3). A graphitic material is determined to be in one of these classifications based on a combination of factors including its G peak position and ratio of D to G peak intensities

The lased GO from Figure 2 appears to be in the nanocrystalline graphite regime due to the low level of dispersion in the G peak. In this regime, the D to G peak intensity varies inversely with the crystallite size L_a according to the following equation:

$$I(D)/I(G) = (C(\lambda))/L_a \qquad\qquad (1)$$

where λ is the energy of the laser (for 633 nm laser, $\lambda = 1.96$ eV) and $C(\lambda) \sim 2.4 \times 10^{-10}\lambda^4$.[3] This provides a crystallite size L_a of ~50-60 nm.

The unlased GO appears to be in stage 2 (due to the high dispersion in the G peak), where the relationship from the equation given above does not apply. However, another phenomenological approach developed by Cancado *et al.*[4] that considers the integrated intensity (peak area) ratios and FWHM of the G band (Gamma_G) can be used to identify the type and concentration of defects that are present. This approach provides a correlation between $(A_D/A_G)E_L^4$ and Gamma_G (E_L =excitation energy) for materials with: 1. only point defects; 2. only line defects; 3. a combination of the two. In addition, it provides a correlation between these two values ($(A_D/A_G)E_L^4$ and Gamma_G) and the domain size within a graphitic material. For materials with mainly line defects, the average domain size is taken to be the crystallite size L_a. For materials with mainly point defects or a combination of the two, the domain size is taken to be the average distance between nearest defects (L_D). Therefore, for a given Raman spectrum, this approach can

be used to first determine what kind of defects dominate, and then to determine the domain size within the material.

The values for $(A_D/A_G)E_L^4$ and Gamma_G for the unlased GO (35 eV[4] and 67 cm^{-1}, respectively) lie in the region predominantly dominated by line defects with a negligible contribution from point defects. Using eq. 1 in Gustavo Cançado *et al*., the domain size is ~7-8 nm.[4] In essence, defects in pristine GO are due to small aromatic cluster size. The values for $(A_D/A_G)E_L^4$ and Gamma_G for the lased GO (10 eV4 and 29 cm^{-1}, respectively) lie in the region where only line defects (at the graphene edges) are present, resulting in an average domain size of L_a ~50-60 nm, which is consistent with the extended graphitic sheets. Using the relationship between $(A_D/A_G)E_L^4$ and Gamma_G from Gustavo Cançado *et al*., the point defect average distance L_D ~ 30 nm is obtained, which suggests a very low density of point densities and of similar order of magnitude as the graphene domains. In lased GO, the nature of the defects and their density, can be independently verified for lased GO, by using the correlation between the ID/IG ratio and ID'/IG provided by Eckmann *et al*.[5] The ratios for the lased GO lie in the region where the graphitic planes are free of vacancies or adatoms. This provides further evidence that the defects in the lased GO are boundaries or edges rather than point defects.

X-ray photoelectron spectroscopy (XPS) Analysis

XPS spectroscopy was performed using a Thermo Scientific K-Alpha + XPS system, using an Al K-alpha source, a 100 μm spot size, and an active electron flood gun. Fine scans of each element were performed using 10 scans, with a dwell time of 25 ms, a pass energy of 50 eV, and a step size of 0.1 eV. Peaks for each spectra were shifted to align with the Si 2p peak at 99.4 eV to compensate for surface charging. SiO_2 and Mn_2O_3 contamination were observed, as verified by the Si 2p and Mn 3s fine scans (Figure S2). The oxygen contribution from these species to the total oxygen concentration was removed from the reported oxygen content in the text.
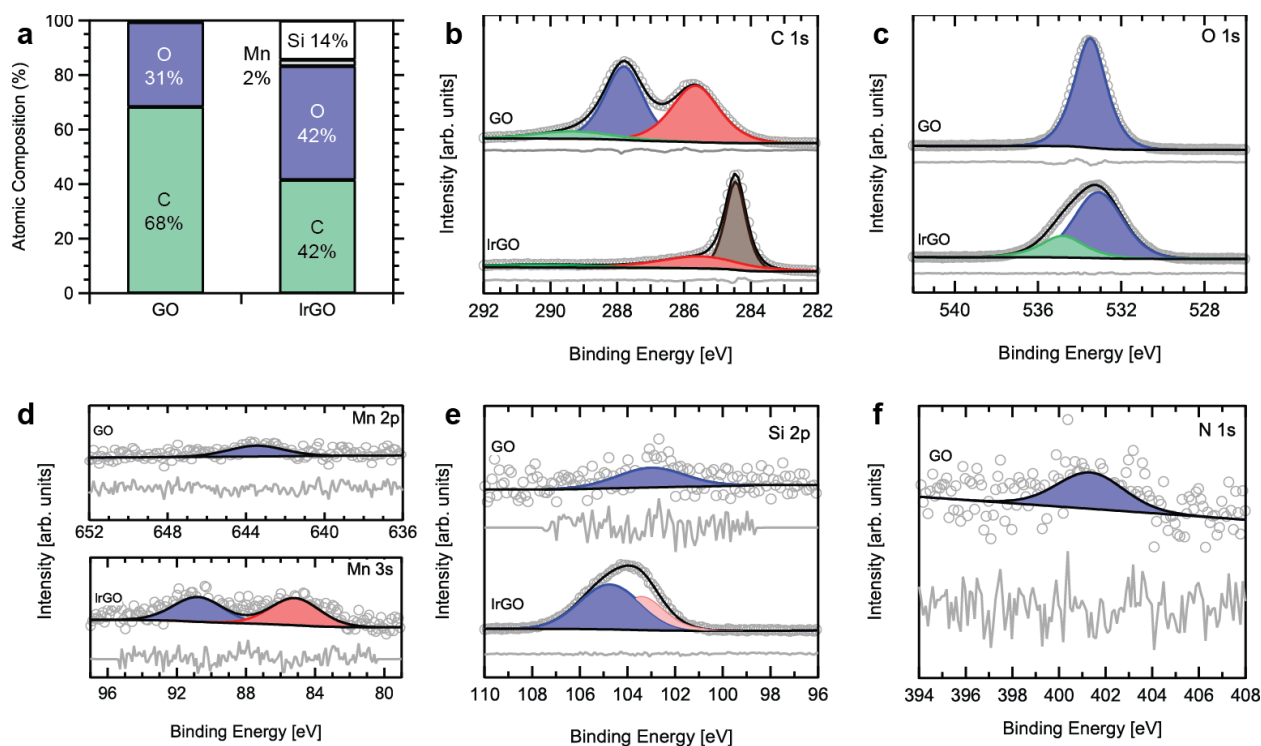
FIGURE S2. (a) Total atomic composition for GO and laser-reduced GO as measured by XPS. Si and Mn become more pronounced after laser pyrolysis, which increases the total oxygen concentration in the lased samples. (b-f) C 1s, O 1s, Mn 2p and Mn 3s, Si 2p, and N 1s spectra for GO and lrGO. No nitrogen was detected for lrGO.

Examination of laser irradiated membranes in SEM

SEM was used to observe the structure of the laser reduced graphene oxide surface as outlined in the Methods section. Particles were observed on the surface in irradiated samples that were not visible on the pristine GO surface (Figure 1). These particles were suspected to be attributable to manganese oxides on the membrane surface, as indicated by XPS.
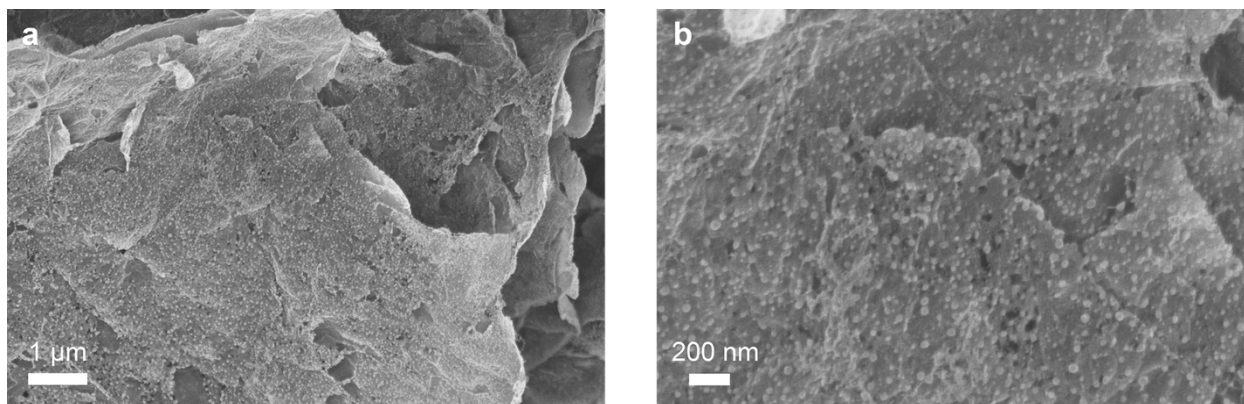
FIGURE S3. SEM images of the laser irradiated graphene surface at (a) 30K and (b) 100K magnifications.

Investigation of particle rejection in laser-reduced GO membranes

Preservation of the underlying pore structure after laser irradiation was investigated in nanoparticle rejection experiments. In these experiments, gold nanoparticle suspensions were filtered through the membrane and the rejection was determined using UV-vis absorption measurements of the feed and permeate. Experiments were conducted using 50 nm and 200 nm gold nanoparticles purchased from Sigma-Aldrich with concentrations of 3.5×10^{10} particles per mL and 1.9×10^9 particles per mL, respectively. Calibration curves relating concentration to absorbance were obtained. The absorbance used for the 50 nm and 200 nm gold nanoparticles was 533 nm and 557 nm, respectively. Rejection experiments were carried out using feed gold nanoparticle suspensions containing 50% dilutions of the stock in DI water.

Gold nanoparticle rejection measurements showed near-identical selectivity in pristine PES membrane and PES membranes with a laser-reduced GO layer. For 200 nm particles, rejection was 79.7% and 78.2% for the pristine PES membranes and PES membranes with a laser-reduced GO layer, respectively. Similar results were found with 50 nm particles, showing 2.4% and 0.3% rejection for pristine PES and PES coated with laser-reduced GO. Overall, the results from rejection tests support observations in SEM showing that the underlying pore structure and selectivity of the membrane is preserved after laser irradiation.